PROVENANCE EVOLUTION AND UNROOFING HISTORY OF A MODERN ARC-CONTINENT COLLISION: EVIDENCE FROM PETROGRAPHY OF PLIO-PLEISTOCENE SANDSTONES, EASTERN TAIWAN[1]

REBECCA J. DORSEY
Department of Geological and Geophysical Sciences
Princeton University
Princeton, New Jersey 08544

ABSTRACT: Plio-Pleistocene sandstones from the Coastal Range of eastern Taiwan provide a record of shifting source areas and unroofing events in adjacent arc and accretionary-wedge terranes during the early stages of arc-continent collision. In latest Miocene and early Pliocene time, arc-derived sediments were deposited in a precollisional forearc basin between the Luzon volcanic arc and the Manila Trench. Sandstones of this age are rich in zoned plagioclase, volcanic lithic fragments, and pelagic foraminifera and contain only minor quartz and sedimentary-metasedimentary lithic fragments. In contrast, lower Pliocene to lower Pleistocene sandstones are poor in feldspar and volcanic fragments and contain abundant sedimentary and metasedimentary lithic fragments. This reflects a provenance shift from the volcanic arc to the uplifted (meta)sedimentary accretionary wedge of proto-Taiwan, which resulted from the early Pliocene onset of arc-continent collision.

A refined classification of sedimentary and metasedimentary lithic fragments is introduced here and used to interpret the early evolution of the collisional orogen. Lithic fragments are rich in pelitic minerals and are divided into: 1) sedimentary (Ls) = mudstone, shale, siltstone, chert and argillite; 2) low-grade metamorphic (Lm1) = slate, slatey siltstone, and quartzite; and 3) medium-grade metamorphic (Lm2) = phyllite-schist, phyllitic quartzite and quartz-mica-albite aggregate. A good correlation is observed between these lithic fragment types and bedrock lithologies exposed in the present-day Central Range of Taiwan. Based on this correlation, the change in relative abundance of sedimentary and metasedimentary lithic fragments through time has been used to interpret an unroofing sequence for the collisional fold-and-thrust belt.

Lower Pliocene Taiwan-derived sandstones are rich in sedimentary lithic fragments (Ls), which were shed from the accretionary wedge during the earliest stages of arc-continent collision. From early Pliocene to early Pleistocene time, sandstones became progressively depleted in Ls lithic fragments and enriched first in Lm1 and later in Lm2 fragments, as deeper levels in the metamorphic complex were uplifted and exposed to erosion. Regional metamorphism of biotite-grade rocks (= Lm2) occurred at about 4.5 Ma at depths of 12–15 km (Ernst 1983) and were uplifted to the surface by about 1.4 Ma (this study). These ages give an uplift rate of 4 to 5 km/m.y., which is in good agreement with independent estimates based on fission-track studies, raised coral reefs, Quaternary elevation changes, and present-day denudation rates. Thus, it appears that sandstone detrital modes of clastic orogenic sequences can be used to interpret specific aspects of unroofing and tectonic evolution in nearby active mountain belts.

INTRODUCTION

The relationship between sandstone composition and plate tectonics has been the subject of intensive research and discussion over the past ten years. Important papers by Dickinson and Suczek (1979), Ingersoll and Suczek (1979), Dickinson and Valloni (1980), Valloni and Mezzadri (1984), and others have contributed to our ability to predict the tectonic setting of a source terrane from framework compositional modes. Limitations of this approach include such problems as temporal changes in tectonic setting (Mack 1984), compositional variations related to depositional environment and climate (Suttner 1974; Mack 1984) and large-scale lateral transport of sand from regions tectonically unrelated to the basin of deposition (Velbel 1985). In spite of these problems, recent workers have been able to recognize unique lithic-fragment detrital modes in sands and sandstones that are derived from uplifted zones of continental collision, or suture belts (Graham et al. 1976; Ingersoll and Suczek 1979; Suczek and Ingersoll 1985). Two ternary diagrams especially useful for identifying sands derived from continental suture belts are 1) polycrystalline quartz—volcanic/metavolcanic lithic fragments—sedimentary/metasedimentary lithic fragments (Qp-Lvm-Lsm); and 2) metamorphic—volcanic—sedimentary lithic fragments (Lm-Lv-Ls). Arc-continent collisions represent a different kind of collisional orogen that may be distinguishable from continent-continent sutures based on QpLvmLsm and LmLvLs detrital modes (Hiscott 1978; Mack 1982).

The purpose of this paper is to document the provenance history of a suite of Plio-Pleistocene sandstones from the Coastal Range of eastern Taiwan. These sandstones are extremely rich in lithic fragments derived from a well-understood Neogene arc-continent collision that is still in progress in Taiwan. In particular, a new classification scheme for sedimentary and low- to medium-grade metamorphic lithic fragments is developed and introduced here. This classification is used, together with independent plate-tectonic, stratigraphic, and petrologic studies, to obtain specific information about the timing and rate of uplift in the collisional metamorphic source.

REGIONAL TECTONIC SETTING AND COASTAL RANGE STRATIGRAPHY

The island of Taiwan is located at the present boundary between the Philippine Sea plate and the Eurasian continent (Fig. 1). It marks the site of an ongoing oblique collision between the west-facing Luzon island arc and the passive continental margin of mainland China. Detailed structural studies and plate reconstructions have shown that the arc-continent collision, which began in early Pliocene time, is propagating to the south along the eastward-dipping Manila Trench at about 85 km/m.y. (Suppe 1980, 1981, 1985; Page and Suppe 1981). Uplift rates determined from Quaternary elevation changes (Bonilla 1977), raised coral reefs (Peng et al. 1979), and

---

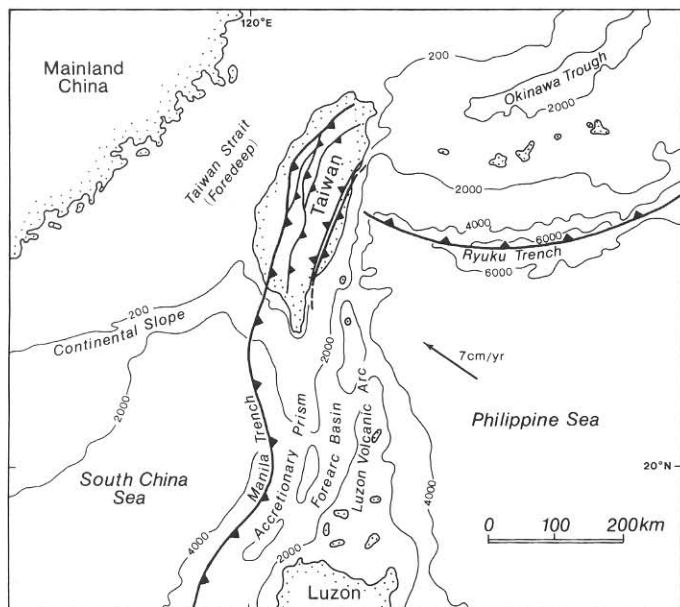[1] Manuscript received 28 October 1986; revised 29 May 1987.

FIG. 1.—Simplified regional bathymetry and tectonic setting of Taiwan, modified after Suppe (1980, 1985). Note the north-trending Luzon volcanic arc and Manila trench that, on the island of Taiwan, are involved in collision with the northeast-trending Chinese continental margin.
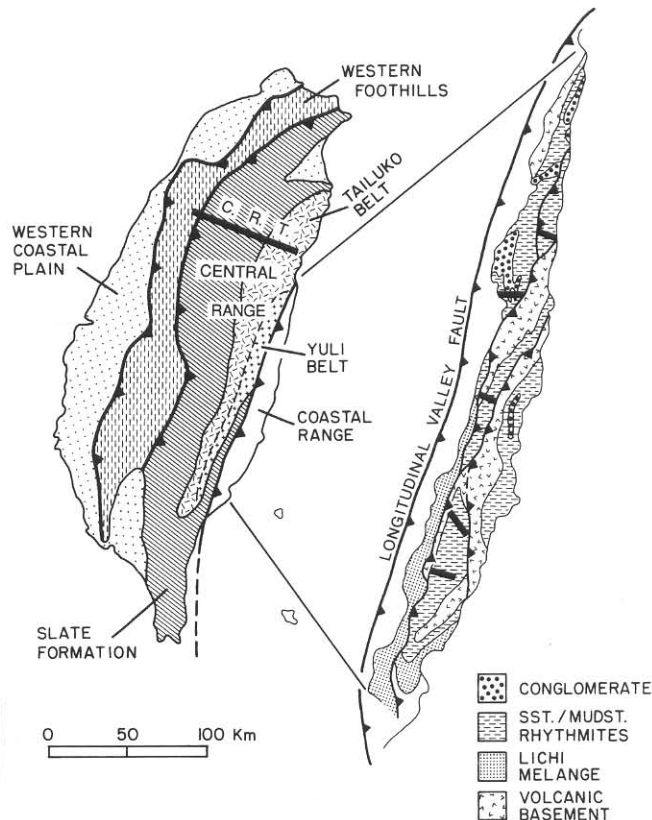

FIG. 2.—Generalized bedrock geology of Taiwan and simplified geologic map of the Coastal Range, modified after Ho (1975) and Chi and others (1981). Transects in the Coastal Range indicate location of sandstone samples collected for this study. Central Range Transect (C.R.T.) shows the area in which samples were collected for analysis of source-terrane lithologies; this is the same area where petrologic and geochemical studies discussed in the text were carried out.

modern denudation rates (Li 1976) average about 5 mm/ yr. These are some of the fastest uplift and denudation rates recorded anywhere in the world (Milliman and Meade 1983) but are probably not uncommon for regions of active mountain building and orogenesis (Zeitler et al. 1982; Adams 1981).

Figure 2 shows the general bedrock geology of Taiwan and a simplified geologic map of the Coastal Range. The Coastal Range is separated from the Central Mountain Range by the currently active Longitudinal Valley Fault. This is an eastward-dipping, low-angle thrust fault that represents a major tectonic suture along which rocks of the volcanic-arc terrane are juxtaposed against an older metamorphic complex with continental affinities (Barrier et al. 1982; Ernst et al. 1985). The Slate Formation and parts of the Western Foothills province represent a thick, shallow-marine clastic wedge that accumulated between Eocene and late Miocene time adjacent to the rifted Chinese continental margin. This eastward-facing clastic wedge became part of the arc-continent collision in early Pliocene time when the buoyant passive margin moved into the Manila Trench (Suppe 1981; Chi et al. 1981).

Sedimentary rocks in the Coastal Range (Fig. 3) are underlain by a volcanic basement complex containing andesites and basaltic andesites, agglomerates, volcanic conglomerates, and bedded tuffs. These basement rocks are part of the Luzon calc-alkaline island arc, which was thrust over the east side of the expanding accretionary wedge in late Pleistocene to Recent time. Overlying the volcanic basement is a thick sequence of clastic sedimentary rocks that range in age from latest Miocene to early Pleistocene (nannofossil zones NN12 to upper NN19). This sequence contains chaotic olistostromes,

mudstones, and pebbly mudstones, rhythmically bedded turbidites and storm-generated tempestites (rhythmites), and coarse cobble-boulder conglomerates (Lundberg and Dorsey 1988). Chi and others (1981) showed that these sediments were deposited rapidly, at rates of 0.3 to 5 km/ m.y., in the Luzon forearc basin prior to and during arc-continent collision.

SANDSTONE PETROGRAPHY

Medium- and coarse-grained sandstones were collected from thin- to thick-bedded sandstone-mudstone rhythmites in five transects across the Coastal Range (Fig. 2). The transects are located in four separate thrust sheets, and mostly comprise homoclinally dipping, continuous stratigraphic sections with little or no disruption by imbricate faults and related folds. One section (second from the south) contains major structural complexities that have not yet been resolved by field mapping. The relative position of sandstones within the composite stratigraphic sequence was determined from nannofossil studies by Chi and others (1981) and Chi (unpubl. data). This provided high-resolution biostratigraphic control essential to making age correlations between different stratigraphic
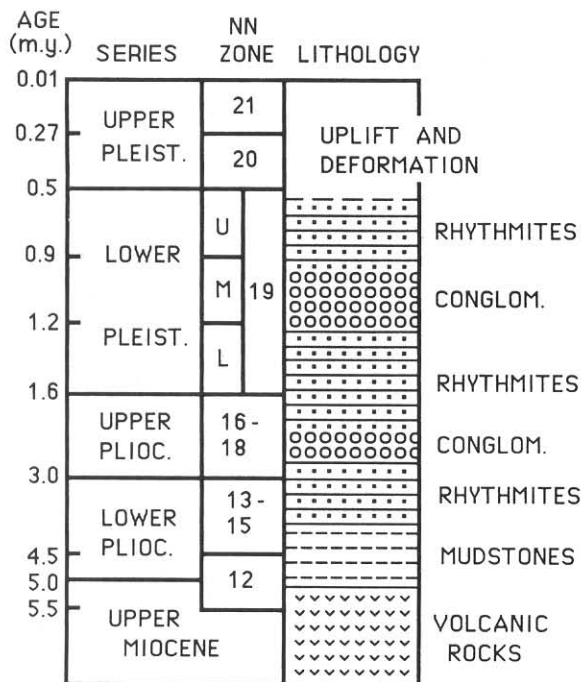
FIG. 3.—Time-stratigraphic chart and simplified lithostratigraphy of Plio-Pleistocene sedimentary rocks in the study area, adapted from Chi and others (1981), Gartner (1977), and preliminary sedimentologic field data. Rhythmites are rhythmically interbedded sandstone-mudstone couplets of both classical turbidites and shallower-water, wave-affected tempestites. Nannofossil (NN) zones are from Chi and others (1981) and Chi (unpubl. data).

TABLE 1.— *Definition of grain parameters*

Q-F-L	Q = Qm + Qp, where:
	Q = total quartz grains
	Qm = monocrystalline quartz
	Qp = polycrystalline quartz
	F = P + K, where:
	F = total feldspar grains
	P = plagioclase, including albite
	K = potassium feldspar
	L = Ls + Lm1 + Lm2 + Lv, where:
	Ls = total sedimentary lithic fragments
	= mudstone + shale + siltstone + chert + argillite
	Lm1 = total low-grade metamorphic lithic fragments
	= slate + quartzite + slatey siltstone
	Lm2 = medium-grade metamorphic lithic fragments
	= phyllite/schist + phyllitic quartzite + qtz-mica-albite aggregate
	Lv = total volcanic lithic fragments
	= vitric + lathwork + felsic + microlitic types
Qm-F-Lt	Qm = moncrystalline quartz
	F = total feldspar
	Lt = total lithic fragments + polycrystalline quartz
Qp-Lvm-Lsm	Qp = polycrystalline quartz
	Lvm = total volcanic and metavolcanic lithic fragments
	= Lv
	Lsm = total sedimentary and metasedimentary lithic fragments
	= Ls + Lm1 + Lm2
Lm-Lv-Ls	Lm = Lm1 + Lm2
	Lv = Lv
	Ls = Ls
Ls-Lm1-Lm2	parameters defined above

sections. The sandstones were thus divided into nanno-fossil-zone age groups, making it possible to document systematic compositional variations through time.

The samples analyzed for this study include only feld-spar-poor, lithic-rich sandstones (Fig. 4A), which contain abundant sedimentary and metasedimentary lithic fragments derived from the collisional accretionary wedge of proto-Taiwan. Twenty-nine thin sections were point-counted for lithic fragments only, including polycrystalline quartz (Qp, Table 1). Feldspar and monocrystalline quartz were not counted because previous studies (Teng 1979; Dorsey 1985a, b) had established reliable QFL and QmFLt modal compositions for these sandstones (see Fig. 6). The results of those studies are discussed below. Three hundred to 400 framework grains were counted per slide on a grid of 0.5 or 1.0 mm, depending on maximum grain size. The Gazzi-Dickinson method of point counting (Ingersoll et al. 1984) was used in order to minimize discrepancies introduced by comparing samples of varying grain size. Because feldspar staining was found to obscure important sedimentary and metamorphic textures within lithic fragments, thin sections were not stained for feldspar.

Potential Limitations

The central purpose of this provenance study was to use temporal variations in sandstone composition to identify changes through time in the type of bedrock li-

thologies exposed in the source area. However, recent workers have pointed out that the relative abundance of unstable minerals and lithic fragments may be greatly reduced by physical and chemical weathering that take place during sediment transport and reworking in the depositional environment (Suttner 1974; Mack 1984). Although this is a severe limitation in some cases, the abundance of unstable sedimentary and metasedimentary lithic fragments in Taiwan-derived sandstones indicates that extensive destruction of labile elements did not occur. Furthermore, the very rapid rates of uplift in Taiwan (5 km/m.y.; Bonilla 1977) and rapid Plio-Pleistocene sedimentation rates (average, 1 to 5 km/m.y.; Chi et al. 1981) both indicate that there was little or no time for sediment storage in destructive fluvial, deltaic, or beach-face environments.

Grain alteration as a result of burial diagenesis was also not a factor in this study. The sandstones that were analyzed are poorly indurated and had to be impregnated with epoxy prior to thin-section preparation. Only minor calcite and silica cements are present, and feldspar grains show little or no alteration except in metamorphic lithic fragments, where pretransportation albitization of plagioclase and potassium feldspar is common. The minor
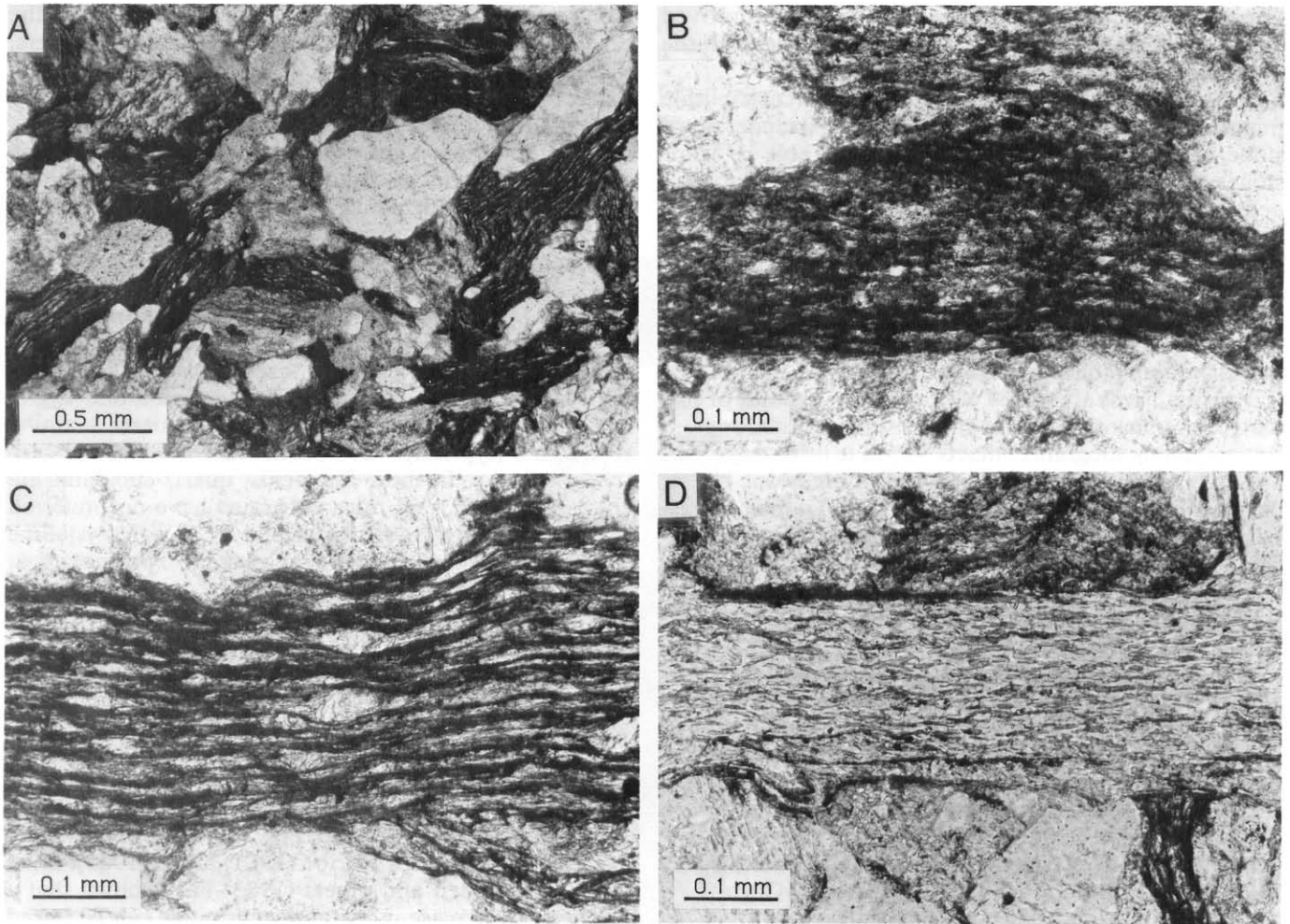
Fig. 4.—Photomicrographs of lithic-rich sandstones from the Coastal Range sequence. A) Typical view of Type-3 sandstone with abundant sedimentary and low- to medium-grade lithic fragments. B) Mudstone fragment (Ls) showing dark, massive clay matrix and unaltered silt. C) Slate fragment (Lm1) with distinctive slatey cleavage, strongly elongate quartz grains, (Lm1) with distinctive slatey cleavage, strongly elongate quartz grains, and opaque carbon(?)-rich zones that alternate with very fine white mica. D) Phyllite-schist lithic fragment (Lm2) showing well oriented, strongly crystalline, fine-grained micas and recrystallized quartz.

amounts of clay matrix present show no signs of early metamorphic sericitization, and clay-rich sedimentary lithic fragments are unaffected by pressure solution at their boundaries or internal recrystallization. The above considerations make it reasonable, for the purposes of this study, to use trends in sandstone detrital modes to interpret evolution of the source terrane through time.

Grain Parameters

The grain parameters used in this study and by Dorsey (1985a) are defined in Table 1. Recognition of quartz and feldspar types was relatively straightforward and followed, for the most part, conventions of Dickinson (1970), Graham and others (1976), and Ingersoll and Suczek (1979). One exception is that chert was included with sedimentary lithic fragments (Ls, Lsm) instead of with polycrystalline quartz (Qp), in order to emphasize the relative abundance of sedimentary versus metamorphic

rocks in the source area. Chert amounted to less than 2–3 percent of the total lithic population in all samples, so this treatment does not significantly affect the results.

A new classification of sedimentary (Ls), low-grade metamorphic (Lm1), and medium-grade metamorphic (Lm2) lithic fragments, based on diagnostic internal sedimentary and metamorphic textures, was developed for this study. This represents a refinement of commonly used petrographic parameters, and it may have widespread application to lithic-rich sandstones shed from other (meta)sedimentary orogenic terranes. Inevitably, increased subjectivity and operator bias are introduced, due to the subtle and sometimes arbitrary distinctions that have to be made between textural features representing a continuum of progressively increasing metamorphic grade. The effect of this can be minimized by masking sample numbers when counting and by consistent application of objective criteria for grain identification. The results presented here indicate that the addi-

tional provenance information gained and the improved ability to interpret unroofing trends greatly outweigh the disadvantages of the method.

Sedimentary Lithic Fragments (Ls).—Sedimentary lithic fragments of Coastal Range sandstones include mudstone, shale, siltstone, argillite, and chert (Table 1). Mudstones (Fig. 4B) are recognized by their dusty-looking, petrographically unresolvable, clay matrix, lack of a preferred planar fabric, and the absence of pressure-solution features in scattered silt subgrains. Shales are characterized by a microscopic planar-bedding fabric that is distinct from the massive fabric of mudstones. Siltstones contain silt- and fine-sand-sized subgrains of subangular to well-rounded quartz, feldspar, and minor, small lithic fragments. These are mixed with variable amounts of clay matrix and lack signs of major pressure solution or grain suturing along subgrain contacts. Argillite lithic fragments have a massive fabric similar to that of mudstone grains, but they contain translucent, very finely grained recrystallized clays up to about 10 microns long. This lithology is transitional to low-grade metamorphic lithic fragments (Lm1) and probably represents the recrystallization of smectites and mixed-layer illite/smectites to illite or sericite at roughly 200°C (Hoffman and Hower 1979).

Low-Grade Metamorphic Lithic Fragments (Lm1).—This class of lithic fragments is a critical intermediate type between sedimentary and medium-grade metasedimentary types. It has not been adequately distinguished from sedimentary and higher-grade metamorphic lithic categories in previous petrographic studies, even though sedimentary and metasedimentary lithic fragments have previously been recognized. Lm1 includes slate, slatey siltstone, and quartzite (Table 1). Slates (Fig. 4C) are characterized by their conspicuous slatey cleavage; this is an undulatory to planar foliation defined by alternating domains of dark, organic(?)-rich clays, very finely grained, recrystallized white mica ± chlorite (average length, 10 to 30 microns), and lenticular grains (or grain clusters) of partially recrystallized quartzo-feldspathic silt and fine sand. Lenticularity and elongation of silt and sand grains are diagnostic of slate fragments. This is apparently a result of pressure solution and, in some cases, local recrystallization of quartz in pressure shadows during lower-greenschist-facies metamorphism.

Quartzite lithic fragments contain partially recrystallized subgrains of quartz ± highly sericitized feldspar ± albite, with minor (< 10%) interstitial recrystallized sericite. Subgrain contacts are commonly sutured, locally to the degree that grain boundaries are poorly defined; the degree of grain suturing and recrystallization is, however, significantly less than that seen in polycrystalline quartz (Qp) and medium-grade metamorphic rock fragments (Lm2). Slatey-siltstone fragments are intermediate between slates and quartzites with respect to the relative abundance of quartz and sericite and commonly exhibit a quartz-sericite "mesh" texture in pressure shadows parallel to the dominant foliation.

Medium-Grade Metamorphic Lithic Fragments (Lm2).—Medium-grade metamorphic lithic fragments are divided into phyllite-schist, phyllitic quartzite, and quartz-mica-albite aggregate. The first two grain types fall into the category of quartz-mica tectonite used by other workers. Phyllite-schist fragments (Fig. 4D) contain clear, euhedral micas that commonly alternate with thin bands of highly recrystallized quartz in a strongly preferred planar metamorphic foliation. Mica grains, although generally finely grained, are distinctly larger than the weakly crystalline sericite in Lm1 fragments, with an average length of 30 to 50 microns. They are composed predominantly of white mica (probably muscovite) ± chlorite ± green and brown biotite.

Phyllitic quartzite lithic fragments contain more than about 75 percent fully recrystallized quartz ± albite, with lesser amounts of well-crystallized micas in a strongly preferred planar orientation. Quartz-mica-albite aggregates consist of nonfoliated, interlocking quartz ± albite, with minor (typically <25%) euhedral white mica, ± biotite ± chlorite. In these fragments, quartz subgrains are equant in shape, and mica subgrains have no preferred orientation; they are distinguished from polycrystalline quartz (Qp) by the presence of at least 3 to 5 percent mica.

Correlation with Bedrock in the Source

A direct correlation can be made between lithic fragments observed in Coastal Range sandstones and equivalent bedrock lithologies in the source terrane of central Taiwan. Bedrock in the Central Range is divided into the western Eocene to middle Miocene Slate Formation and the eastern pre-Tertiary metamorphic complex called the Tananao Schist (Ho 1975; Fig. 2). Recent petrographic and petrologic studies by Liou (1981), Chen (1981), Ernst (1983), and Chen and others (1983) have shown that a progressive increase in metamorphic grade can be traced across the Central Range from the westernmost part of the Slate Formation to the central part of the Tananao metamorphic basement complex. This metamorphic sequence ranges from zeolite facies in the west, through prehnite-pumpellyite and lower-greenschist facies (chlorite zone), into middle-greenschist facies (biotite zone) of the Tananao Schist. The observed assemblages represent a close approach to chemical equilibrium that was attained synchronously across the Central Range during a recrystallization event associated with the early Pliocene arc-continent collision (Ernst 1983).

As part of the current study, a representative suite of sedimentary and metamorphic rocks was collected from a transect across the Central Range in the same area studied by the above-mentioned authors (see Fig. 2). Indurated sandstones, shales, and argillites of the westernmost Slate Formation (zeolite facies) correspond to sedimentary (Ls) lithic fragment types as described above. A wide belt of chlorite-grade slates and quartzites occupies the eastern three quarters of the Slate Formation; these rocks contain distinctive slatey cleavage, elongate quartz grains, fine-grained sericite and chlorite, and other low-grade metamorphic textures and minerals identical to the ones found in Lm1 lithic fragments. Finally, the transition into the Tananao Schist is characterized by the occurrence of biotite-bearing phyllites and quartz-mica schists contain-
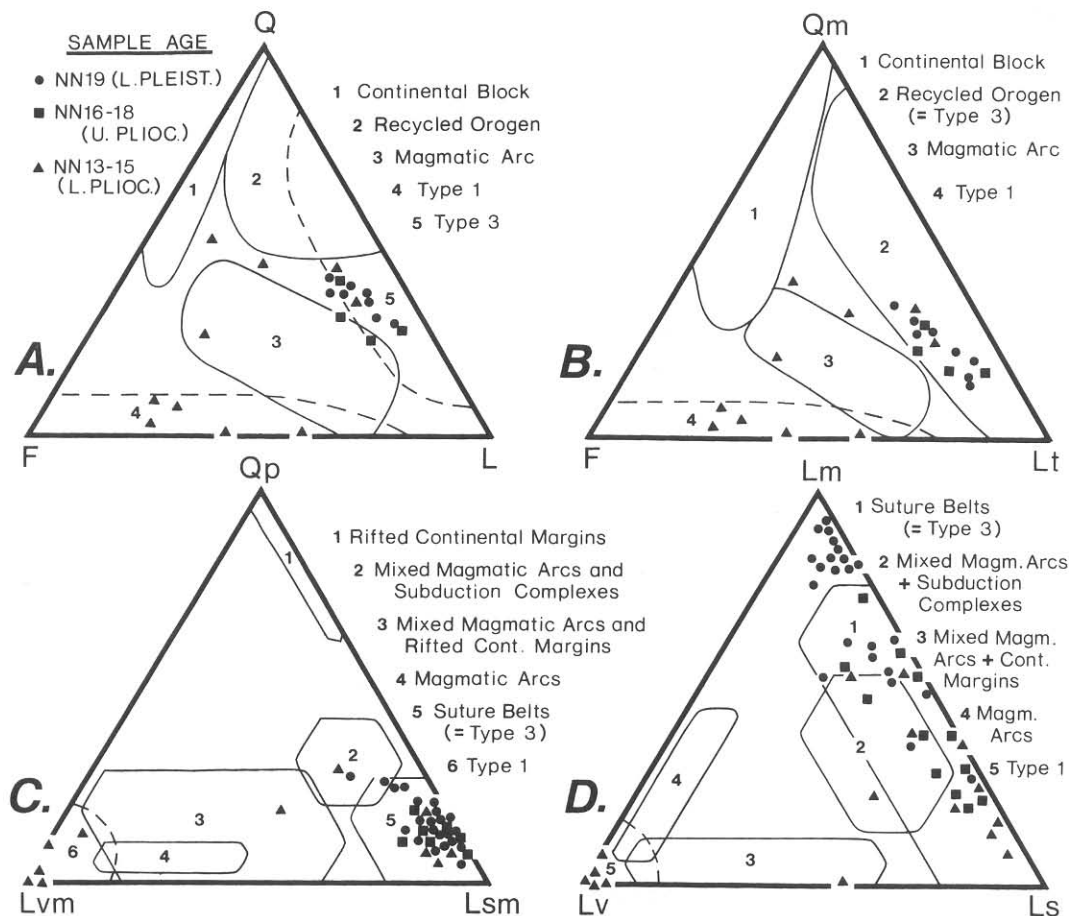
FIG. 5.—Ternary diagrams of Coastal Range sandstones. A (QFL) and B (QmFLt) are from Dorsey (1985a); C (QpLvmLsm) and D (Lm-LvLs) plot data from Dorsey (1985a) and this study. Provenance fields are from Dickinson and Suczek (1979) and Ingersoll and Suczek (1979); Type 1 and Type 3 are from Teng (1979). In general, the data fall into two clusters: 1) quartz-poor, feldspar-rich sandstones with abundant volcanic lithic fragments, all early Pliocene in age; and 2) feldspar- and volcanic-fragment-poor lithic arenites, ranging in age from early Pliocene to early Pleistocene, which contain moderate amounts of quartz and abundant sedimentary-metasedimentary lithic fragments. The age and compositional grouping represents a shift in source areas from the Luzon volcanic arc to the proto-Taiwan accretionary wedge that resulted from the early Pliocene onset of arc-continent collision (see Fig. 7).

ing Lm2-type medium-grade metamorphic textures; these include well-developed planar foliation, strongly crystalline micas (muscovite, ± biotite, chlorite), and extensively recrystallized quartz.

RESULTS

The results of framework modal analysis of Taiwan-derived sandstones are presented in Table 2. In Figure 5, these data and those of Dorsey (1985a) are plotted in four ternary diagrams (QFL, QmFLt, QpLvmLsm, and LmLvLs). Figure 6 is a new triangular diagram for modal analysis of sedimentary (Ls), low-grade metamorphic (Lm1), and medium-grade metamorphic (Lm2) lithic fragments. This plot was used, together with independent information about the timing and conditions of collision-related metamorphism, to determine the rate of Plio-Pleistocene uplift and unroofing in the (meta)sedimentary source terrane. The following sections examine each of the ternary diagrams in light of the provenance information they provide, with particular emphasis on the new LsLm1Lm2 plot.

Early Provenance Shift

In Figure 5, the data are divided into three nannofossil zones according to biostratigraphic studies by Chi and

others (1981) and Chi (unpubl.): NN13-15 (lower Pliocene), NN16-18 (upper Pliocene), and NN19 (lower Pleistocene). In both the QFL and QmFLt diagrams (Fig. 5A, B), most of the data fall into two clusters. One cluster is restricted in age to the early Pliocene; these sandstones contain minor quartz and abundant feldspar and volcanic lithic fragments. Dorsey (1985a) obtained modal averages of Q8-F60-L32 and Qm6-F60-Lt34 for this group, which was first recognized and named Type 1 by Teng (1979). These sandstones commonly contain zoned plagioclase, pelagic foraminifera (globigerina), and fragments of coralline limestone derived from fringing reefs on the volcanic arc. Chi and others (1981) found that Type-1 sandstones accumulated relatively slowly (0.3 to 0.5 km/m.y.) in a forearc basin adjacent to the Luzon volcanic arc, prior to its early Pliocene collision with the Chinese continental margin. Other workers have recently shown that this composition of sandstone is especially common in sedimentary basins that form on the flanks of intra-oceanic island arcs (Valloni and Mezzadri 1984).

The second group of sandstones contains little feldspar and abundant sedimentary and metasedimentary lithic fragments (Fig. 5), and corresponds to Type 3 of Teng (1979). Framework modal averages determined by Dorsey (1985a) are Q34-F12-L54 and Qm24-F12-Lt64. These sandstones range from early Pliocene to early Pleistocene in age and were derived from the accretionary fold-and-
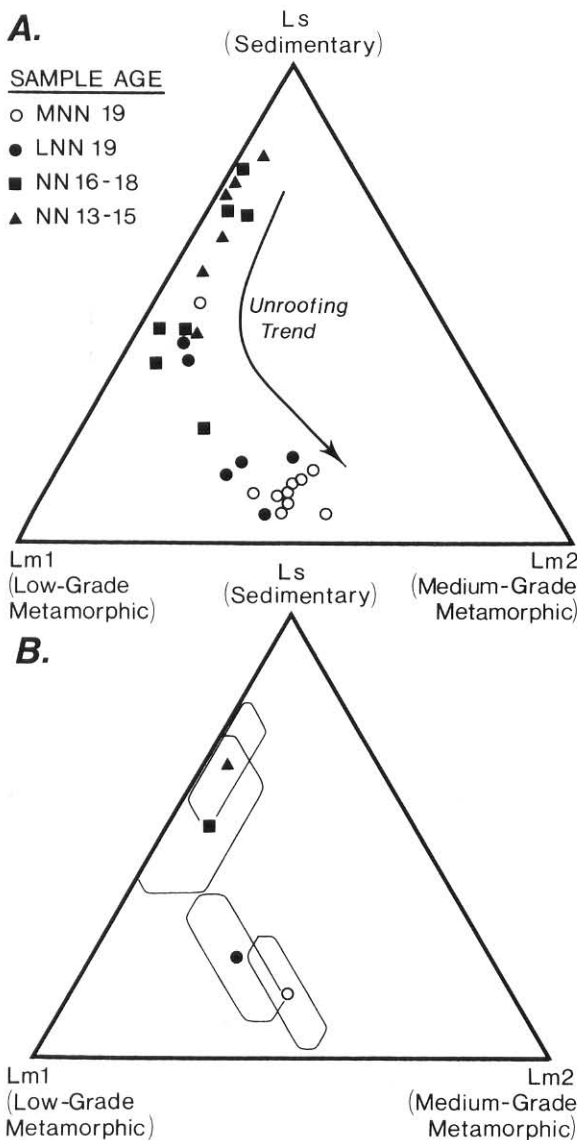
A.

B.

Fig. 6.—Ternary diagram of lithic fragments defined in this paper: sedimentary (Ls); low-grade metamorphic (Lm1); and medium-grade metamorphic (Lm2). A) Distribution of sandstones within a well-defined compositional field. Note that the oldest samples plot near the Ls corner, and younger samples become progressively enriched first in Lm1 and later in Lm2. B) Same diagram plotting means and standard deviations of each age group. Note the strong age dependence of the compositional trend; this reflects unroofing of the (meta)sedimentary complex through time and erosion into progressively deeper (higher-grade) levels in the collision belt.

TABLE 2.—*Means and standard deviations of lithic fragments in Coastal Range sandstones analyzed for this study*

Nannofossil Zone	% Qp-Lvm-Lsm			% Lm-Lv-Ls			% Ls-Lm1-Lm2		
	Qp	Lvm	Lsm	Lm	Lv	Ls	Ls	Lm1	Lm2
NN13-15 (n = 6)									
Mean	9	4	87	32	4	64	67	29	4
Std. dev.	4	4	5	14	4	15	14	12	3
NN16-18 (n = 7)									
Mean	11	4	85	46	5	50	52	40	8
Std. dev.	3	4	5	19	5	19	20	15	7
L. NN19 (n = 6)									
Mean	13	2	85	75	2	22	23	50	27
Std. dev.	3	2	4	15	2	13	15	5	15
M. NN19 (n = 10)									
Mean	10	4	86	82	5	13	14	44	42
Std. dev.	3	3	4	13	4	12	12	4	13
L. and M. NN19 (n = 16)									
Mean	12	3	85	80	4	16	17	46	37
Std. dev.	4	3	3	14	4	13	14	5	15

end of major sediment input from the Luzon volcanic arc and the beginning of rapid uplift and erosion of the Taiwan collisional orogen to the west (Page and Suppe 1981; Chi et al. 1981).

A third, poorly defined field of lower Pliocene sandstones is represented by three points on QFL and QmFLt diagrams (Fig. 5A, B). This framework composition was recognized and named Type 2 by Teng (1979). Type-2 sandstones, which were not examined in detail for this study, are typically rich in fine and very finely grained detrital quartz, with subordinate feldspar and lithic fragments. This represents early collisional recycling of unlithified quartz-rich sediment that was shed from the highest parts of the accretionary prism, prior to erosion into deeper structural levels containing cemented and metamorphosed sedimentary rocks.

LsLm1Lm2 Diagram

The data in Figure 6A are divided according to age into four different nannofossil zones ranging from lower Pliocene (NN13-15) to the middle part of the lower Pleistocene (middle NN19). This diagram reveals a well-developed compositional field falling close to the Ls-Lm1 tie line, which bends away from this line toward the Lm1-Lm2 join. Closer inspection shows that the oldest samples fall in the Lm2-poor part of the field, concentrated near the Ls corner. Successively younger samples first become enriched in Lm1 lithic fragments and then in Lm2 fragments, with Ls content progressively decreasing through time. With one exception, all of the youngest samples (middle NN19) are restricted to the Ls-depleted domain where Lm1 and Lm2 are subequal. This trend reflects the progressive stripping away of a sedimentary cover sequence and erosion into successively higher-grade metamorphic rocks during uplift and unroofing of the collisional fold-and-thrust belt.

In order to display better this time-dependent com-

thrust belt of Taiwan during arc-continent collision. On a QpLvmLsm ternary diagram (Fig. 5C), these sandstones cluster tightly into the provenance field of suture belts defined by Ingersoll and Suczek (1979). On a plot of LmLvLs (Fig. 5D), they fill the provenance field of suture belts, with older sandstones plotting near the sedimentary (Ls) corner and younger samples falling near the metamorphic (Lm) corner. The age and petrographic data plotted in Figure 5 reveal a pronounced shift in the composition of Coastal Range sandstones that occurred in the early Pliocene (NN13-15). This shift marks the virtual

positional trend, the data in Figure 6B are replotted using a method introduced by Ingersoll (1978) and further developed by Ingersoll and Suczek (1979). In this diagram, the mean of each group is plotted at a point in the middle of a polygon representing ± one standard deviation for each variable. A systematic unroofing trend through time is again evident.

RATE OF PLIO-PLEISTOCENE UPLIFT

In order to constrain the rate of uplift and unroofing in the metamorphic source, we need to know the conditions (or depth) and timing of metamorphism in the source terrane, as well as the time at which major surface erosion of the metamorphic terrane first occurred. Whereas the conditions of Pliocene metamorphism are relatively well known (Ernst 1983), the age of this event in Taiwan is still somewhat problematic. Plate kinematic and stratigraphic studies are currently the most reliable for dating the onset of collision-related metamorphism in central Taiwan. A geometric analysis of the oblique, southward-propagating arc-continent collision shows that the collision began in northern Taiwan about 4 Ma (Suppe 1981). This is supported by high-resolution stratigraphic studies of eastern Taiwan (Chi et al. 1981) and western Taiwan (Chang and Chi 1983), which showed that the earliest sediments derived from the uplifted collision belt are 3.5 to 4.0 million years old (early Pliocene). Furthermore, a recent study of clay mineralogy in the Coastal Range sequence showed that mudstones as old as 4.5 m.y. contain abundant illite and chlorite that were derived from proto-Taiwan during the earliest stages of collision-related uplift (Buchovecky 1986). The onset of this collision is widely recognized to coincide with Pliocene regional metamorphism of basement and cover rocks exposed in the Central Range today (Stanley et al. 1981; Ho 1982).

Isotopic age determinations for this metamorphic event show considerably more variation and inconsistency. Law and Aronson (1983) obtained K-Ar dates of 5 to 10 m.y. from phyllites and schists in the Central Range, which they recognized as being generally too old due to inherited excess argon. Jahn and others (1986) obtained mineral isochron Rb-Sr ages from granites of the Tailuko Belt ranging from 2.5 to 6.5 Ma, as well as one K-Ar biotite age of 4.2 Ma. High-pressure mafic rocks from the Yuli Belt in the easternmost Central Range yield Rb-Sr ages of about 4.6 Ma, but due to structural complications are probably not representative of the overall metamorphic history of the region (Jahn et al. 1981). A further complication lies in the fact that metamorphism in Taiwan is an ongoing process that is probably occurring at depth today beneath the Central Range. Therefore, metamorphic dates from the Tananao Schist are expected to be younger than those of the as yet undated metamorphic detritus contained in Plio-Pleistocene sediments of the Coastal Range sequence. These problems indicate that, until more reliable geochemical data become available, the plate kinematic and stratigraphic studies referred to above provide the most reliable estimate for the timing

TABLE 3.—*Calculation of uplift rate*

TIMING of collision-related metamorphism, based on plate kinematic and stratigraphic studies (Suppe 1981; Chi et al. 1981; Buchovecky 1986), about 4.5 Ma.

CONDITIONS of metamorphism, based on petrology and geochemistry of metamorphic rocks in the Central Range (Ernst 1983),

Lm1: T = 325° ± 75°C   P = 3 kbar (chlorite grade)
Lm2: T = 425° ± 75°C   P = 4 kbar (biotite grade).

DEPTH of metamorphism: Modern geothermal gradient in western Taiwan (Suppe and Witke 1977) = 30°C/km. Assuming lithostatic gradient of about 3 km/kbar, depth of Lm2 metamorphism = 12–15 km.

TIMING of surface erosion of biotite-grade (Lm2) metamorphic rocks based on ternary Ls-Lm1-Lm2 diagram (this paper), about 1.4 Ma (= midpoint of lower NN19).

RATE of uplift: Biotite-grade metamorphic rocks uplifted from 12–15 km depth to the surface between about 4.5 and 1.4 m.y. (= 3.1 m.y.): Uplift rate = 3.9 to 4.8 km/m.y.

of early collision-related metamorphism in Taiwan, at about 4.5 Ma.

The temperature and pressure conditions, which give an estimate of the depth of metamorphism in the Central Range, are relatively well known. In a petrologic study of metamorphic rocks in the Central Range, Ernst (1983) found that the physical conditions of recrystallization at moderate activities of H_2O and CO_2 were as follows: 1) in the eastern part of the Slate Formation (= Lm1), T = 325° ± 75°C, P = 3 kbar; and 2) in the Tananao basement complex (= Lm2), T = 425° ± 75°C, P = 4 kbar. Using the modern geothermal gradient in western Taiwan of 30–35°C/km (Suppe and Wittke 1977) and a standard lithostatic gradient of about 3 kbar/km, we obtained an equilibration depth for the biotite-grade Tananao schist of between 12 and 15 km.

Based on the tectonic, stratigraphic and petrologic studies cited above, and the sandstone petrographic data in Figure 6, it is now possible to derive a Plio-Pleistocene uplift rate for metamorphic rocks in the collisional accretionary wedge. The calculation used for this determination is outlined in Table 3. Peak metamorphism occurred in the basement and cover rocks of the Central Range sometime in the early Pliocene, probably around 4.5 Ma. By the beginning of early Pleistocene time (lower NN19, midpoint = 1.4 Ma), significant areas of middle-greenschist-facies rocks (Lm2) were exposed at the surface and were being eroded and transported into the adjacent collisional basin to the east. This represents uplift of the basement complex from 12–15 km depth to the surface over a period of about 3.1 m.y., which is equivalent to an uplift rate of approximately 4–5 km/m.y.

The uplift rate derived above is in good agreement with numerous other independent assessments of uplift in Taiwan. Liu (1982) measured fission-track ages of zircon, apatite, and sphene from the Tananao Schist and obtained rates of uplift ranging from 4.2 to 6.8 mm/yr (km/m.y.) for the time interval between 3.0 and 0.5 Ma. Lee (1977) used the abundance of slate fragments in Plio-Pleistocene sandstones of western Taiwan to infer that uplift rates in
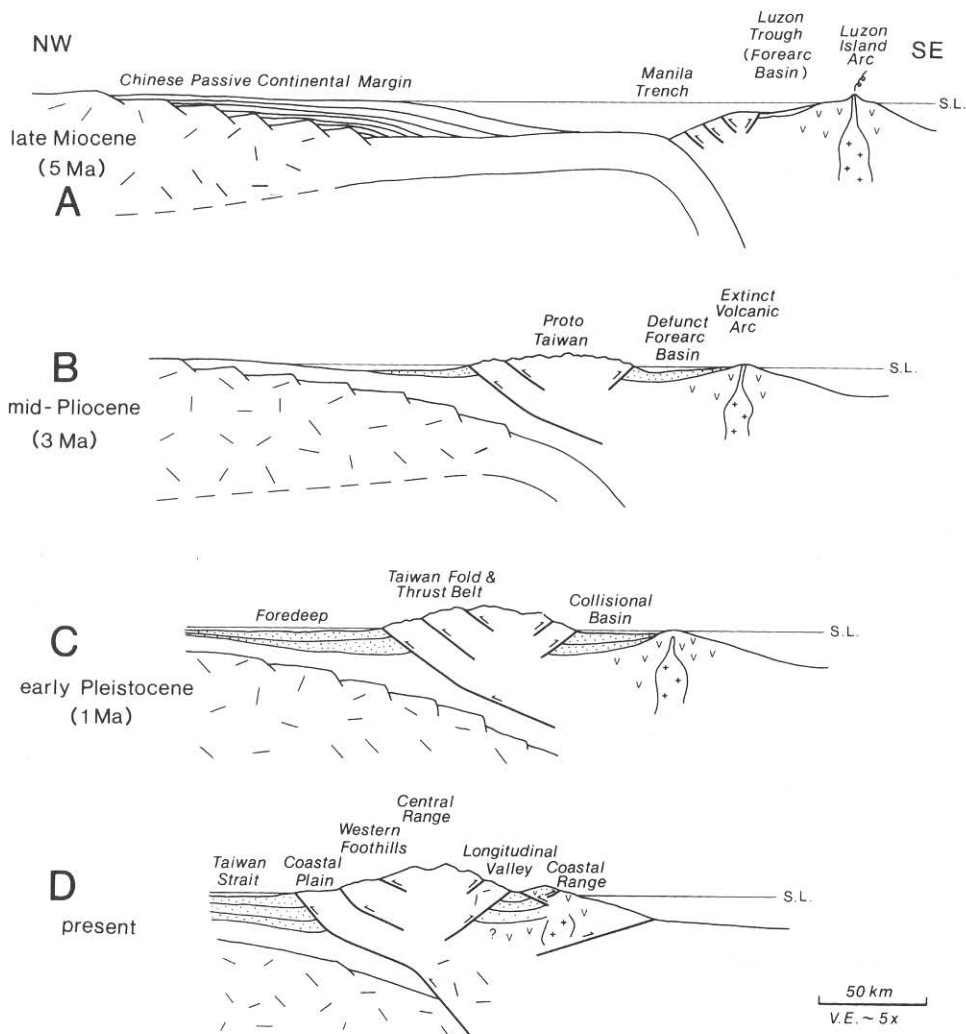
FIG. 7.—Schematic diagram showing the tectonic evolution of the Taiwan collisional orogen from late Miocene time to the present, based on studies by Suppe (1981), Covey (1984), Lundberg and Dorsey (1988), and this paper. Sandstones analyzed for this study were deposited in the Luzon forearc basin, which continued subsiding and evolved into a collisional basin during the Plio-Pleistocene. A rapid shift from a volcanic-arc source terrane (A) to one in the uplifted accretionary wedge (B) took place in the early Pliocene in response to the onset of arc-continent collision. C) The provenance shift was followed by rapid uplift (4–5 km/m.y.) and unroofing of the (meta)sedimentary fold-and-thrust belt during late Pliocene and early Pleistocene time. D) From late Pleistocene time to the present, volcanic and sedimentary rocks in the collisional basin were uplifted and thrust over the accretionary wedge to their present position in the Coastal Range. Figure adapted from Lundberg and Dorsey (1988).

the Slate Formation increased exponentially between 3 and 1 Ma, averaging about 5 mm/yr. Radiocarbon dates of Holocene-raised coral reefs in southern and eastern Taiwan yield consistent values of 5.0 ± 0.7 mm/yr (Peng et al. 1977). Furthermore, estimates of modern uplift rates in Taiwan that are based on present-day denudation (Li 1976) and Quaternary elevation changes (Bonilla 1977) give similar rates of about 5 mm/yr.

DISCUSSION

Evolution of Arc-Continent Collision

Detailed petrographic analysis of Plio-Pleistocene sandstones from eastern Taiwan provides information about the evolution of the arc-continent collision, which is schematically illustrated in Figure 7. During late Miocene time (5–10 m.y.), the Luzon island arc existed in a pre-collisional setting above subducting ocean crust of the South China Sea (Fig. 7A). Quartz-poor calcareous sandstones containing abundant zoned plagioclase and volcanic lithic fragments were deposited in the forearc basin. Figure 7B depicts initial early Pliocene collision of

the volcanic arc with the Chinese continental margin and its thick clastic wedge. This resulted in rapid uplift of the accretionary prism and cessation of major volcanic activity in the arc. During this early collision stage, middle-greenschist-facies metamorphism was occurring at depth in the accretionary wedge and underlying rocks of the continental basement. At the surface, unlithified sediment and unmetamorphosed sedimentary rocks (Ls) were being eroded and transported into the collisional forearc basin. Active erosion and detrital input from the Luzon volcanic arc had, for the most part, ended.

Late Pliocene and early Pleistocene evolution of the collisional orogen (Fig. 7C) was characterized by rapid uplift (4 to 5 km/m.y.) in the accretionary wedge and erosion into progressively deeper levels in the sedimentary-metasedimentary complex. As a result, sandstones in the collisional basin to the east became enriched first in low-grade metamorphic lithic fragments (Lm1) and later in medium-grade fragments (Lm2) that were derived from lower- and middle-greenschist-facies rocks in the source area. During the late Pleistocene and Holocene, volcanic basement rocks and overlying orogenic sediments of the collisional basin were thrust westward along

the Longitudinal Valley suture to their present position in the Coastal Range (Fig. 7D).

Comparison with Ancient Sandstones

The Taiwan-derived lithic-rich sandstones that were analyzed for this study contain only very minor amounts of volcanic lithic fragments. On QpLvmLsm and Lm-LvLs ternary diagrams, they fall well within provenance fields normally attributed to derivation of sediment from a continent-continent suture (Fig. 5C, D; Ingersoll and Suczek 1979). In this respect, they do not resemble the intermediate-composition sandstones containing mixed volcanic, quartzose, and (meta)sedimentary detritus, which were deposited in the Appalachian foredeep and derived from arc-continent collisions during the Ordovician (Hiscott 1978) and Carboniferous (Mack 1982, 1984). This is especially enigmatic because the Plio-Pleistocene collisional basin was developed between the growing accretionary wedge of Taiwan to the west and the dying volcanic arc to the east (Fig. 7). The paucity of volcanic detritus in these sandstones apparently resulted from an early Pliocene, regional subsidence event in the volcanic arc that coincided with rapid uplift of the newly exposed and expanding accretionary wedge (Lundberg and Dorsey 1988). The area of arc rocks exposed above sea level, as well as overall relief on the arc system, were greatly reduced at that time, effectively cutting off much of the Luzon island arc as an active source of sediment. The volcanic basement complex and overlying collisional-basin sediments continued to subside during the Plio-Pleistocene, with rapid input to the basin of quartz-rich (meta)sedimentary detritus from the accretionary wedge that strongly diluted the slow input from the arc.

During the late Pleistocene to Recent, however, the collisional basin was strongly telescope, uplifted, and accreted to the eastern part (Coastal Range) of the Taiwan collision zone, where large areas of the volcanic-arc basement are now exposed. As the arc-continent collision evolves in the future, we can predict that volcanic rocks in the Coastal Range will be structurally incorporated into the metamorphic core of the mountain belt by imbricate thrusting toward the west. This mixed volcanic and metamorphic terrane will probably have a high positive relief similar to the Central Range in Taiwan today, with major river systems draining both to the east and west. These rivers will then be likely to transport sand of intermediate composition westward into the foredeep, analogous to the sandstones analyzed by Hiscott (1978) and Mack (1982, 1984). Thus, the discrepancy between sandstone compositions in the eastern Taiwan collisional basin (this study) and those of the Paleozoic Appalachian foredeep can be explained by the very early stage of Plio-Pleistocene arc-continent collision in Taiwan compared to the advanced stage of collision reflected in sandstones of the Appalachian foredeep.

CONCLUSIONS

Plio-Pleistocene sandstones in the Coastal Range were deposited in a forearc basin that subsided rapidly and evolved into a collisional basin during the initiation and early development of arc-continent collision in Taiwan. Sandstone detrital modes reflect a dramatic provenance shift from the intra-oceanic Luzon volcanic arc to the subaerially exposed and expanded accretionary prism that coincided with the onset of the collision. Arc-derived sandstones are rich in zoned plagioclase, volcanic lithic fragments, and pelagic foraminifera. In contrast, sandstones derived from the accretionary wedge contain abundant (meta)sedimentary lithic fragments, moderate quartz, and only minor feldspar; their framework composition is indistinguishable from that of sands derived from continent-continent collisions. A progressive decrease through time in sedimentary lithic fragments (Ls), and increase first in low-grade (Lm1) and later in medium-grade (Lm2) metamorphic lithic fragments, provide evidence for uplift and unroofing of the accretionary wedge. The timing of this unroofing trend in the sandstones has been combined with independent estimates for the timing and conditions of metamorphism in the source to estimate the rate of uplift in the collision zone, at 4–5 km/m.y.

The method introduced here for determining uplift rates in a metamorphic source terrane based on sandstone petrography is new and has not been attempted in previously reported studies. Independent estimates of uplift in Taiwan constitute a test of the method, and the results are encouraging. The applicability of this technique to other synorogenic sandstones will probably depend on several factors. These include the following: 1) burial history of the sandstones and degree of lithic-fragment alteration; 2) recognition of rock fragments that show a systematic increase in metamorphic grade; 3) reliable age dates for the sandstones; and 4) integrated stratigraphic, petrologic, and geochemical data for the conditions and timing of metamorphism in the source. These requirements may be reasonable for clastic sequences deposited adjacent to other modern and ancient mountain belts. In fact, the approach that is outlined here may find useful applications in areas where a metamorphic source terrane has been largely eroded away, leaving behind only a stratigraphic record of its unroofing history.

REFERENCES

ADAMS, C. J., 1981, Uplift rates and thermal structure in the Alpine Fault zone and Alpine Schists, southern Alps, New Zealand, in McKay, K. R., and Price, N. J., eds., Thrust and Nappe Tectonics: Geol. Soc. London Spec. Publ. No. 9, p. 211–222.

BARRIER, E., ANGELIER, J., CHU, H. T., AND TENG, L. S., 1982, Tectonic analysis of compressional structures in an active collision zone: the deformation of the Pinanshan conglomerates, eastern Taiwan: Proc. Geol. Soc. China, v. 25, p. 123–138.

BONILLA, M. G., 1977, Summary of Quaternary faulting and elevation changes in Taiwan: Geol. Soc. China Mem., No. 2, p. 43–55.

BUCHOVECKY, E. J., 1986, Clues to the development of the Taiwan orogen from mudstones of the southern Coastal Range [unpubl. senior thesis]: Princeton University, 32 p.

CHANG, S. S. L., AND CHI, W. R., 1983, Neogene nannoplankton biostratigraphy in Taiwan and the tectonic implications: Petroleum Geology of Taiwan, No. 19, p. 93–147.

CHEN, C. H., 1981, Change of x-ray diffraction pattern of K-micas in the metapelites of Taiwan and its implication for metamorphic grade: Geol. Soc. China Mem. No. 4, p. 475–490.

CHEN, C. H., CHU, H. T., LIOU, J. G., AND ERNST, W. G., 1983, Explanatory notes for the metamorphic facies map of Taiwan: Central Geol. Survey Spec. Publ. No. 2, Taipei, Taiwan, R.O.C., 32 p.

CHI, W. R., NAMSON, J., AND SUPPE, J., 1981, Stratigraphic record of plate interactions in the Coastal Range, eastern Taiwan: Geol. Soc. China Mem. No. 4, p. 155–194.

COVEY, M., 1984, Lithofacies analysis and basin reconstruction, Plio-Pleistocene western Taiwan foredeep: Petr. Geology of Taiwan, No. 20, p. 53–83.

DICKINSON, W. R., 1970, Interpreting detrital modes of graywacke and arkose: Jour. Sed. Petrology, v. 40, p. 695–707.

DICKINSON, W. R., AND SUZCEK, C. A., 1979, Plate tectonics and sandstone compositions: Am. Assoc. Petroleum Geologists Bull., v. 63, p. 2164–2182.

DICKINSON, W. R., AND VALLONI, R., 1980, Plate settings and provenance of sands in modern ocean basins: Geology, v. 8, p. 82–86.

DORSEY, R. J., 1985a, Petrography of Neogene sandstones from the Coastal Range of eastern Taiwan: Response to arc-continent collision: Petr. Geol. Taiwan, No. 21, p. 187–215.

———, 1985b, Petrography of Neogene sandstones, eastern Taiwan: Response to arc-continent collision: Geol. Soc. America Abstr. w. Progr., v. 17, p. 565.

ERNST, W. G., 1983, Mineral parageneses in metamorphic rocks exposed along Tailuko Gorge, Central Mountain Range, Taiwan: Jour. Metamorphic Geology, v. 1, p. 305–329.

ERNST, W. G., HO, C. S., AND LIOU, J. G., 1985, Rifting, drifting, and crustal accretion in the Taiwan sector of the Asiatic margin, in Howell, D. G., ed., Tectonostratigraphic Terranes of the Circum-Pacific Region, circum-Pacific Council for Energy and Mineral Resources: Earth Science Series, Vol. 1, p. 375–389.

GARTNER, S., 1977, Calcareous nannofossil biostratigraphy and revised zonation of the Pleistocene: Marine Micropaleontology, v. 2, p. 1–25.

GRAHAM, S. A., INGERSOLL, R. V., AND DICKINSON, W. R., 1976, Common provenance for lithic grains in Carboniferous sandstones from Ouachita Mountains and Black Warrior Basin: Jour. Sed. Petrology, v. 46, p. 620–632.

HISCOTT, R. N., 1978, Province of Ordovician deep-water sandstones, Tourelle Formation, Quebec, and implications for initiation of the Taconic Orogeny: Can. Jour. Earth Sci., v. 15, p. 1579–1597.

HO, C. S., 1975, An Introduction to the Geology of Taiwan—Explanatory Text of the Geologic Map of Taiwan: Ministry of Economic Affairs, Republic of China, Taipei, 153 p.

HOFFMAN, J., AND HOWER, J., 1979, Clay mineral assemblages as low grade metamorphic geothermometers: application to the thrust faulted disturbed belt of Montana, U.S.A., in Scholle, P. A., and Schluger, P. R., eds., Aspects of Diagenesis: Soc. Econ. Paleontologists Mineralogists Spec. Publ. No. 26, p. 55–79.

INGERSOLL, R. V., 1978, Petrofacies and petrologic evolution of the Late Cretaceous forearc basin, northern and central California: Jour. Geology, v. 86, p. 335–352.

INGERSOLL, R. V., AND SUCZEK, C. A. 1979, Petrology and provenance of Neogene sand from Nicobar and Bengal Fans, DSDP sites 211 and 218: Jour. Sed. Petrology, v. 49, p. 1217–1228.

INGERSOLL, R. V., BULLARD, T. F., FORD, R. L., GRIMM, J. P., PICKLE, J. D., AND SARES, S. W., 1984, The effect of grain size on detrital modes: A test of the Gazzi-Dickinson point-counting method: Jour. Sed. Petrology, v. 54, p. 103–116.

JAHN, B. M., LIOU, J. G., AND NAGASAWA, H., 1981, High-pressure metamorphic rocks of Taiwan: REE geochemistry, Rb-Sr ages, and tectonic implications: Geol. Soc. China Mem., No. 4, p. 497–520.

JAHN, B. M., MARTINEAU, F., PEUCAT, J. J., AND CORNICHET, J., 1986, Geochronology of the Tananao Schist complex, Taiwan, and its regional tectonic significance: Tectonophysics. v. 125, p. 103–124.

LAW, E., AND ARONSON, J. L., 1983, The argillaceous Cenozoic geosyncline of Taiwan, source and age of metamorphism: Geol. Soc. America Abstr. Progr., v. 15, p. 624.

LEE, P. J., 1977, Rate of the early Pleistocene uplift in Taiwan: Geol. Soc. China Mem., No. 2, p. 71–76.

LI, Y.-H., 1976, Denudation of Taiwan Island since the Pliocene epoch: Geology, v. 4, p. 105–107.

LIOU, J. G., 1981, Recent high CO_2 activity and Cenozoic progressive metamorphism in Taiwan: Geol. Soc. China Mem., v. 4, p. 551–581.

LIU, T. K., 1982, Tectonic implication of fission track ages from the Central Range, Taiwan: Geol. Soc. China Proc., No. 25, p. 22–37.

LUNDBERG, N., AND DORSEY, R. J., 1988, Synorogenic sedimentation and subsidence in a Plio-Pleistocene collisional basin, eastern Taiwan, in Kleinspehn, K. L., and Paola, C., eds., New Perspectives in Basin Analysis: New York, Springer-Verlag, p. 265–280.

MACK, G. H., 1982, Composition of Carboniferous sandstones in the Black Warrior Basin: Implication on plate-tectonic setting, inThomas, W. A., and Neathery, T. L., eds., Appalachian Thrust Belt in Alabama: Tectonics and Sedimentation: New Orleans, La., Geol. Soc. America Guidebook for Fieldtrips No. 13, p. 67–78.

———, 1984, Exceptions to the relationship between plate tectonics and sandstone compositions: Jour. Sed. Petrology, v. 54, p. 212–220.

MILLIMAN, J. D., AND MEADE, R. H., 1983, Worldwide delivery of river sediment to the oceans: Jour. Geology, v. 91, p. 1–21.

PAGE, B. M., AND SUPPE, J., 1981, The Pliocene Lichi Melange of Taiwan: its plate tectonic and olistostromal origin: Am. Jour. Sci., v. 281, p. 193–227.

PENG, T. H., LI, Y. H., AND WU, F. T., 1977, Tectonic uplift of the Taiwan island since the early Holocene: Geol. Soc. China Mem., No. 2, p. 57–69.

STANLEY, R. S., HILL, L. B., CHANG, H. C., AND HU, H. N., 1981, A transect through the metamorphic core of the Central Mountains, southern Taiwan: Geol. Soc. China Memoir, No. 4, p. 443–473.

SUCZEK, C. A., AND INGERSOLL, R. V., 1985, Petrology and provenance of Cenozoic sand from the Indus Cone and Arabian Basin, DSDP sites 221, 222, and 224: Jour. Sed. Petrology, v. 55, p. 340–346.

SUPPE, J., 1980, A retrodeformable cross section of northern Taiwan: Proc. Geol. Soc. China, v. 23, p. 46–55.

———, 1981, Mechanics of mountain building and metamorphism in Taiwan: Geol. Soc. China, Mem. No. 4, p. 67–89.

———, 1985, Kinematics of arc-continent collision, flipping of subduction and back-arc spreading near Taiwan: Geol. Soc. China Mem., No. 6, p. 21–33.

SUPPE, J., AND WITTKE, J. H., 1977, Abnormal pore-fluid pressures in relation to stratigraphy and structure in the active fold-and-thrust belt of northwestern Taiwan: Petr. Geol. Taiwan, No. 14, p. 11–24.

SUTTNER, L. J., 1974, Sedimentary petrographic provinces: an evaluation, in Ross, C. A., ed., Paleogeographic Provinces and Provinciality: Soc. Econ. Spec. Publ. No. 21, p. 75–84.

TENG, L. S., 1979, Petrographical study of Neogene sandstones of the Coastal Range, eastern Taiwan (1. Northern Part): Acta Geol. Taiwan, No. 20, p. 129–155.

VALLONI, R., AND MEZZADRI, G., 1984, Compositional suites of terrigenous deep-sea sands of the present continental margins: Sedimentology, v. 31, p. 353–364.

VELBEL, M. A., 1985, Mineralogically mature sandstones in accretionary prisms: Jour. Sed. Petrology, v. 55, p. 685–690.

ZEITLER, P. K., TAHIRKHELI, R. A. K., NAESER, C. W., JOHNSON, N. M., 1982, Unroofing history of a suture zone in the Himalaya of Pakistan by means of fission-track annealing ages: Earth Planet. Sci. Lett., v. 57, p. 227–240.